

(SSEs) burning liquid oxygen and hydrogen (LOX/LH₂) but with an improved thermal protection system. The expendable ET would be made from new lightweight materials that provide adequate strength and lower cost. The reusable SRBs, now designated redesigned solid rocket motors (RSRMs), would be recovered after launch for reuse. The primary use of the Shuttle II would be that of placing the largest or heaviest payloads (up to about 52,000 lb) in low orbit and of providing a large orbital spacecraft for special extended missions with a large complement of astronauts.

The Mini I is the largest minishuttle with a $\frac{3}{4}$ -size reusable orbiter and a $\frac{3}{4}$ -size expendable ET. It would have a single LRE (RD-180) burning liquid oxygen and kerosene (LOX/RP-1). The reusable SRBs would be the same RSRMs used with the Shuttle II. The primary use of the Mini I would be that of placing large payloads (up to about 38,000 lb) in low orbit more cheaply than the Shuttle II and of providing a less costly spacecraft for certain manned missions with fewer astronauts. It could also be used in various ways for support of the International Space Station (ISS).

The Mini II is a smaller version of the Mini I with a $\frac{1}{2}$ -size reusable orbiter and a $\frac{3}{5}$ -size expendable ET. Like the Mini I it has a single LRE (AJ26-58) burning liquid oxygen and kerosene (LOX/RP-1). The expendable SRBs would be the same SRMs used as boosters for the Titan III SLV. The primary use of the Mini II would be that of placing medium payloads (up to about 21,000 lb) in low orbit more cheaply than in using the larger vehicles and of providing a relatively inexpensive spacecraft for small manned missions. It could also be used as a low-cost space ferry to transport personnel and cargo to or from the ISS.

The Mini III is an even smaller version of the Mini I with a $\frac{1}{3}$ -size reusable orbiter and a $\frac{2}{5}$ -size expendable ET. It also has a single LRE (LR87-AJ-11), but both oxidizer and fuel (N₂O₄/Aerozine-50) are noncryogenic and hypergolic. The expendable SRBs would be similar to the Titan III SRMs used with the Mini II but reduced in size by a scale factor of 0.825. With use of storable bipropellant, the vehicle could be maintained in a launch-ready condition for extended periods of time. The primary use of the Mini III would be that of ferrying personnel to or from the ISS, in space rescue situations where a quick response is necessary, and in serving as a military spacecraft for the U.S. Air Force.

The nominal payloads listed in Table 1 are for low Earth orbit. For higher orbits the size of payload would have to be reduced, or additional propellant would be required. To increase the amount of liquid propellant for the Mini I, the volume of the ET would have to be increased. An alternative procedure for the smaller Mini II and Mini III would be to also add segments to the SRBs. Thus, a modular approach to increasing the amounts of solid and liquid propellants could be developed for each vehicle to provide greater flexibility in performance.

Conclusions

Launch vehicle architecture derived from the space shuttle and modified slightly would be a sure and practical alternative to advanced architectures being studied by NASA in its Space Launch Initiative. Such alternative architecture could include a second-generation shuttle and several minishuttles of various size using noncryogenic fuel. Because all of these launch vehicles would use existing and proven propulsion systems, development time and cost would be considerably less than with any of the architectures being considered in the Space Launch Initiative. Moreover, if the cost of expendable components used with each of the minishuttles were to be a small fraction of recurring launch costs, there could be significant reductions in specific payload costs (that is, launch costs per pound of payload) from prevalent values in the launch vehicle industry. Thus, there is good reason for NASA and the U.S. Department of Defense to consider the alternative architecture in meeting their needs for reliable, cost-effective space transportation in the early 21st century.

References

- ¹Morring, F., Jr., "NASA Tacks Away From X-33 in Space Launch Initiative," *Aviation Week and Space Technology*, Vol. 154, No. 21, 2001, pp. 30–32.
- ²Morring, F., Jr., "NASA Looks Beyond Big Boys for SLI Ideas," *Aviation Week and Space Technology*, Vol. 154, No. 5, 2001, pp. 59, 60.

³Isakowitz, S. J., Hopkins, J. P., Jr., and Hopkins, J. B., *International Reference Guide to Space Launch Systems*, 3rd ed., AIAA, Reston, VA, 1999, pp. 39–470.

⁴Nelson, D. A., "The Case for Shuttle II," *Aerospace America*, Vol. 31, No. 11, 1993, pp. 24–27.

⁵Boltz, F. W., "Payload Capability of Kerosene-Fueled Mini Shuttle," *Journal of Spacecraft and Rockets*, Vol. 34, No. 5, 1997, pp. 685–687.

⁶Boltz, F. W., "Mini/Micro Shuttles with Hypergolic Noncryogenic Liquid Rocket Bipropellant," *Journal of Spacecraft and Rockets*, Vol. 36, No. 4, 1999, pp. 605–608.

J. A. Martin
Associate Editor

Simplified Algorithm for Short Target-Approach Paths in Orbit

Hans F. Meissinger* and David Diaz†
Microcosm, Inc., El Segundo, California 90245

Nomenclature

a_{cor}	=	Coriolis acceleration, m/s ²
a_r	=	centripetal acceleration, m/s ²
r_c	=	local curvature radius of transfer arc in relative motion, m
s	=	arc length of single transfer arc, m
s_i	=	line segment of single transfer arc, m
s_t	=	total transfer distance along target approach direction, $n s_i$, m
t	=	elapsed transfer time, s
t_T	=	total transfer time, s
V	=	relative departure velocity (magnitude) of transfer arc, m/s
V_r	=	velocity of circular reference orbit, m/s
x, y, z	=	horizontal, radial and normal relative motion components, respectively, of transfer arc m
$\dot{x}, \dot{y}, \dot{z}$	=	corresponding relative velocity components, m/s
α	=	initial velocity angle relative to selected approach direction, deg
Δt_i	=	time required for single transfer arc, s
ΔV_i	=	velocity change required at end of each single transfer arc, m/s
θ	=	reference orbit central angle traversed during time t , ωt , deg
ω	=	angular rate of circular reference orbit, rad/s

Subscript

0	=	initial value
---	---	---------------

Introduction

SERVICING, support, and resupply of space systems, whether manned or unmanned, are becoming increasingly important space mission objectives.^{1,2} These types of support missions will play an important role in the operation of the International Space Station (ISS) and must be performed often. The orbital dynamics of the target approach and the maneuvering activity required to achieve this objective are generally referred to as "proximity operations" and have been extensively covered in the literature, including

Received 29 October 2001; revision received 4 June 2002; accepted for publication 10 July 2002. Copyright © 2002 by Hans F. Meissinger and David Diaz. Published by the American Institute of Aeronautics and Astronautics, Inc., with permission. Copies of this paper may be made for personal or internal use, on condition that the copier pay the \$10.00 per-copy fee to the Copyright Clearance Center, Inc., 222 Rosewood Drive, Danvers, MA 01923; include the code 0022-4650/02 \$10.00 in correspondence with the CCC.

*Engineering Consultant. Associate Fellow AIAA.

†System Engineer, System Engineering Division.

Refs. 1–13. The orbital rendezvous equations published in 1960 by Clohessy and Wiltshire³ (C–W) are based on a linearized version of the basic Keplerian equations of motion of a chaser vehicle relative to a target vehicle, to provide a good approximation of the exact solution over distances of several hundred kilometers. Their applicability and usefulness are discussed in the literature (including Refs. 1, 2, 4, 6, and 7). Actually, the linearized form of close-distance relative motion equations was first published by G. S. Hill in 1878, but their designation as C–W equations is currently in common use.

The close, final approach of the space shuttle or an orbital transfer vehicle to a target spacecraft such as the ISS typically is designed to follow a sequence of short, shallow near-circular arcs with radii that are determined by their initial velocity. This brief transfer phase requires a small transverse maneuver at the end of each short arc. A representative final approach sequence is shown in Fig. 1a, in accordance with NASA instruction manuals^{12,13} for approaches to the target spacecraft, for example, for ISS resupply visits. The final approach to the ISS can be performed in the so-called *V*-bar or *R*-bar direction, along (or opposite to) the orbital velocity or the orbital radius direction, respectively. Figure 1a illustrates the *R*-bar approach.

The objective of this Note is to introduce a very simple algorithm, not published previously, for determining the target approach at very close distances, of the order of 100 m or less, with sufficiently high accuracy. It requires only a small amount of computational effort compared to the C–W equations.³ This algorithm allows quick-look target approach calculations in preliminary mission design but can

also be used in actual flight control during that phase. The new approximation technique is based on equating the Coriolis and the centrifugal effects acting on the vehicle during the short time interval during which the magnitude of the relative velocity along a target approach arc segment remains very nearly constant. Typically, with approach segments of only few minutes duration, each covering up to 20- or 30-m distance, the results obtained by this simplified algorithm are quite accurate, with approximation errors of relative positions and velocities with respect to the target typically less than 1%, as shown by the detailed error analysis data presented in this Note.

To visualize the basis of the approximation being used, consider an elliptical relative motion around a reference object, after departure in radial direction from a given, nearby coaltitude position. The initial relative motion can be closely approximated by an inscribed (osculating) circle. Calculating parameters of this circle is a much simpler task than solving the C–W equations.³

Approximation Algorithm

Note from Fig. 1a that the final approach of an orbit transfer vehicle or the Space Shuttle Orbiter to a target vehicle consists of a series of short near-circular arcs. (This final transfer may be preceded by longer approach arcs, typically in the *V*-bar direction, that may last for a whole orbital revolution. That transfer cannot be approximated by the simplified algorithm proposed here because it extends over relatively long distances and time intervals.) The proposed simplified algorithm for each of the final target approach arcs is based on equating the Coriolis acceleration $a_{cor} = 2\omega V$, acting normal to the angular velocity vector ω and the path velocity vector V , with the centripetal acceleration $a_r = V^2/r_c$, where r_c is the local radius of curvature. This means that the inward pointing Coriolis effect is balanced by the centrifugal effect acting in opposite direction. For the small time intervals considered here, the velocity magnitude V is assumed to be constant.

For each transfer arc in the approach sequence equating a_{cor} and a_r and, hence, setting $2\omega V = V^2/r_c$, yields

$$r_c = V/(2\omega) \quad (1)$$

This and the other parameters of the short circular arc, as shown in Fig. 1b, can then be derived as follows: For a given departure angle α , the line segment s_i between the arc's endpoints A and B is determined by

$$s_i = 2r_c \sin \alpha \quad (2)$$

Substituting r_c from Eq. (1) leads to

$$s_i = V(\sin \alpha)/\omega \quad (3)$$

where α typically is of the order of 6–12 deg. The actual arc length s between A and B , based on the assumed constant velocity V , is given by the product $2\alpha r_c$ and, hence, by the use of Eq. (1) again,

$$s = V\alpha/\omega \quad (4)$$

(with α measured here in radians). The time interval between A and B can then be derived, that is,

$$\Delta t_i = s/V = \alpha/\omega \quad (5)$$

To start the next equal-size segment beyond point B , with the same initial path velocity and the same departure angle α as before, a velocity change is required that is given by

$$\Delta V_i = 2V \sin \alpha \cong 2V\alpha \quad (6)$$

To stop the final approach sequence when arriving at the designated target point, a retromaneuver of the same magnitude as the departure velocity V is required. To complete the approach sequence of n segments, with the total length $s_T = ns_i$ requires a total time that is given by ns/V but can be obtained in good approximation by

$$t_T = ns_i/V = s_i/V \quad (7)$$

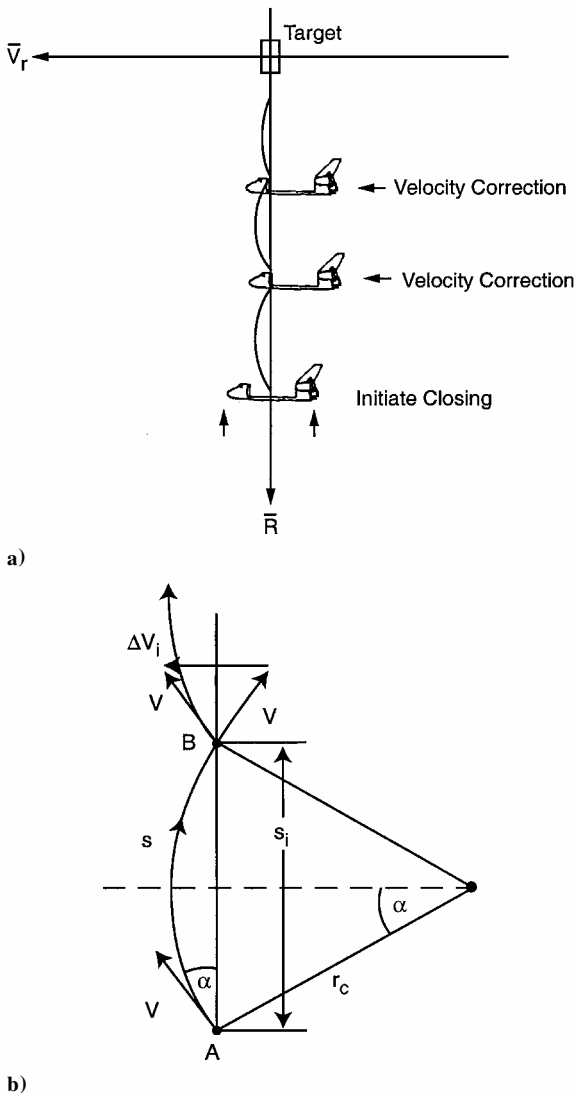


Fig. 1 Representative final approach path of space shuttle to a target object^{12,13}: a) typical *R*-bar approach sequence and b) approximate circular approach segment *AB* and geometrical characteristics.

From these equations, the characteristics of a final target approach in the *V*-bar or *R*-bar direction are determined for a given initial target distance and the number of arc segments. Figure 2 shows the

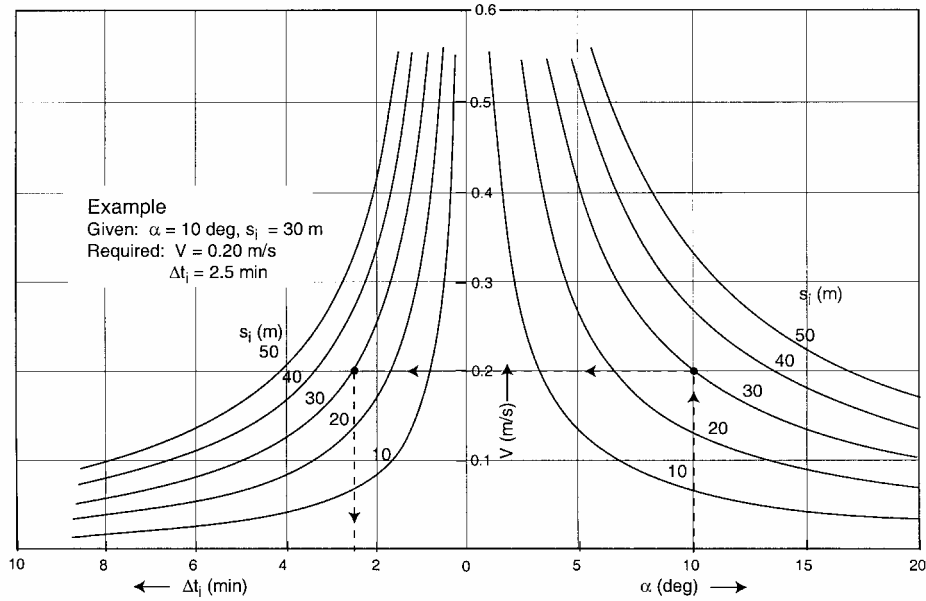


Fig. 2 Velocity and time interval vs departure angle and segment length (for 300-km reference orbit altitude, with $\omega = 1.157 \times 10^{-3}$ rad/s).

relationships between the parameters α , s_i , V , and Δt_i as derived from Eqs. (3) and (5) and indicates the high sensitivity of the latter two parameters to the selected values of α and s_i .

Approximation Accuracy

To determine the approximation error of the short, circular arc with an assumed constant path velocity, as defined by Eqs. (1–5), the more exact solution of the C–W equations³ for the same initial conditions will be used as a reference. For transfers in the orbit (x, y) plane with excursions in x counted positive in the direction opposite the orbital velocity and excursions in y positive in the radially outward direction (in accordance with Refs. 1, 2, 3, and 7) the C–W equations³ in the x – y plane are given by

$$x = 2(\dot{x}_0/\omega - 3y_0) \sin \omega t - (2\dot{y}_0/\omega) \cos \omega t + (6y_0 - 3\dot{x}_0/\omega)\omega t + x_0 + 2\dot{y}_0/\omega \quad (8)$$

$$y = (2\dot{x}_0/\omega - 3y_0) \cos \omega t - (\dot{y}_0/\omega) \sin \omega t + 4y_0 - 2\dot{x}_0/\omega \quad (9)$$

with zero excursions z normal to the orbit plane. When initial values x_0 , y_0 , and \dot{x}_0 , \dot{y}_0 are assumed and the angular rotation rate ω for a given orbital altitude is used, the time history for any specific target approach trajectory can be derived by using these equations.

As a simple accuracy test of the assumed constant path velocity V , a single arc originating at $x_0 = 0$ and $y_0 = 0$ in the horizontal (V -bar) direction, with $\dot{y}_0 = 0$, is assumed. In this case, Eqs. (8) and (9) reduce to

$$x = (\dot{x}_0/\omega)(4 \sin \omega t - 3\omega t), \quad y = (2\dot{x}_0/\omega)(\cos \omega t - 1) \quad (10)$$

The velocity components \dot{x} and \dot{y} , required to determine the relative velocity time history $V(t) = (\dot{x}^2 + \dot{y}^2)^{1/2}$ then become

$$\dot{x} = \dot{x}_0(4 \cos \omega t - 3), \quad \dot{y} = -2\dot{x}_0 \sin \omega t \quad (11)$$

For a single arc, again originating at the origin, but in a radial (R -bar) direction, that is, $\dot{x}_0 = 0$, Eqs. (8) and (9) reduce to

$$x = (2\dot{y}_0/\omega)(1 - \cos \omega t), \quad y = (\dot{y}_0/\omega) \sin \omega t \quad (12)$$

$$\dot{x} = 2\dot{y}_0 \sin \omega t, \quad \dot{y} = \dot{y}_0 \cos \omega t \quad (13)$$

Table 1 lists the change in the actual flight-path velocity $V(t)$ relative to the assumed constant velocity and the relative approximation error as functions of the time elapsed. The second column lists the path angle $\theta = \omega t$ along the circular reference orbit, the third column the relative velocity variation, and the fourth column the relative velocity error, as counted from the reference point, $x = 0$ and $y = 0$. However, because of arc segment symmetry on both sides

Table 1 Approximation error, assuming constant path velocity vs transfer time along near-circular arc (for V -bar and R -bar transfers)

Time of half-arc t , s	Path angle ωt , deg	Velocity ratio ^b V_t/V	Velocity error $\Delta(V_t/V)$, %
<i>V-bar transfer</i>			
60	3.98	1.000037	0.004
120	7.95	1.000472	0.047
180	11.93	1.00277	0.277
240	15.91	1.00900	0.900
300	19.89	1.02113	2.113
<i>R-bar transfer</i>			
60	3.98	1.00719	0.719
120	7.95	1.0259	2.59
180	11.93	1.0622	6.22
240	15.91	1.1070	10.70
300	19.89	1.1607	16.07

^aReference orbit altitude is 300 km. ^b V_t is time-varying velocity.

of the reference point, the resulting velocity variations can actually be counted over time intervals that are twice as large as those given in column 1. These results indicate that the velocity variation is less than 1% up to 8 min for the total arc length in the first case (V -bar departure) and up to 2.5 min for the second case (R -bar departure).

As a more representative test case, the relative position and velocity errors were determined for three-segment, 60-m transfers in the V -bar and R -bar approach directions, with each arc segment being 20 m long. With an assumed departure angle of 10 deg and a departure velocity of 13.32 cm/s, the transfer time per arc, as determined by the simplified algorithm, is 2.5 min in both cases. By the use of the more precise Eqs. (8) and (9) for calculating the reference trajectory characteristics, the approximation errors of the simplified algorithm were determined at the endpoints of each of the three approach path segments.

The times of reaching these endpoints were dictated by the instant the reference trajectory arc intersects the approach direction line, that is, the x axis in the V -bar approach case and the y axis in the R -bar approach case. This means that there were small approximation errors in x positions in the V -bar approach case (or y positions in the R -bar case), in velocity magnitude V and in actual endpoint arrival time. These approximation errors are listed in Table 2 for the three endpoints of each of the two alternate approach directions. The results show that the maximum error values of position, velocity, and total transfer time are of the order of 1% or less in the V -bar, and 5% or less in the R -bar approach case. The different error magnitudes in the two approach directions correspond to those noted earlier for the simpler velocity error evaluation (Table 1).

Table 2 Approximation errors in three-segment approach examples in V-bar and R-bar directions^a

Segment endpoint	Time error		Position error		Velocity error	
	s	%	cm	%	cm/s	%
<i>V-bar approach</i>						
1	3.0	1.96	6.0	0.30	0.0503	0.378
2	6.0	1.96	12.0	0.30	0.1012	0.758
3	9.0	1.96	18.0	0.30	0.1520	1.141
<i>R-bar approach</i>						
1	6.0	3.85	31.6	1.58	0.612	4.59
2	12.0	3.85	72.8	1.82	0.641	4.81
3	18.0	3.85	153.0	2.55	0.705	5.29

^a Assumed 10-deg departure angle and 20-m segment length. Reference orbit altitude 300 km.

It is important to recognize that, during the final target approach phase, some small measurement and execution errors are inevitable. These can be of the same order of magnitude as the approximation errors inherent in the proposed simplified algorithm. It is reasonable, therefore, to make use of this algorithm to control or correct the immediate and subsequent trajectory execution steps. Approach safety constraints can, thus, be met instantly by continuous assessment of the effect of a departure from the initially planned final approach conditions.

Conclusions

The simple algorithm presented here offers a major reduction of computational effort associated with determining the characteristics (e.g., the correction maneuvers ΔV_i) of multisegment chaser-to-target approach paths of the type currently postulated in target rendezvous and docking approaches. The approximation also will be useful in comparing approach modes or different specific characteristics in the process of conducting actual rendezvous and docking missions rather than the more precise solution of the C-W equations.³ Determination of the detailed time history of each approach segment is unnecessary, and the time interval for its completion is explicitly known on the basis of the other transfer arc parameters. The approximation errors are sufficiently small to be of little concern for the short distances and time intervals considered during the final rendezvous and docking approach. In particular, using the C-W equations as an alternative to determine all parameters of interest requires more extensive calculations based on assumed segment lengths and transfer times or the initial velocity components in the x and y directions.

Of particular interest is the quick-look determination of approach path changes and terminal conditions reached resulting from various velocity magnitude and direction changes. Determination of approach path characteristics and effects of any parameter changes can be of major importance, even during the final minutes of an actual rendezvous mission, for example, if unforeseen conditions require a modification of the approach mode. This assessment can be of major concern in meeting overall safety constraints and determining required approach-phase protection procedures. These and other advantages are relevant in justifying the simplified terminal flight-path algorithm described here.

Acknowledgments

The authors appreciate the encouragement and practical suggestions they received from J. R. Wertz, G. Gurevich, T. Bauer, and J. Collins of Microcosm, Inc., in developing the technique described here and assessing its applicability and usefulness.

References

- Waltz, D. M., *On-Orbit Servicing of Space Systems*, Krieger Publishing Co, Malabar, FL, 1993.
- Meissinger, H. F., Section on Proximity Operations, Supplement to *On-Orbit Servicing of Space Systems* by D. M. Waltz, Krieger, Malabar, FL, 1998, pp. 313–317.
- Clohesy, W. R., and Wiltshire, R. S., "Terminal Guidance System for Satellite Rendezvous," *Journal of the Aero/Space Sciences*, Vol. 27, No. 9, 1960, pp. 653–658 and 674.

⁴Wolverton, E. O. (ed.), *Flight Performance Handbook for Orbital Operations*, Wiley, New York, 1961, Chap. 4.

⁵Kaplan, M. H., *Modern Spacecraft Dynamics and Control*, Wiley, New York, 1976, Chap. 3.6.

⁶Dunning, R. S., "The Orbital Mechanics of Flight Mechanics," NASA SP-325, 1973, Chap. 3.

⁷Meissinger, H. F., "Satellite Proximity Operations Near a Shuttle or a Future Space Station," 1983 Annual Conference of Hermann-Oberth-Gesellschaft, Koblenz, Germany, Sept. 1983.

⁸Wertz, J. R., *Spacecraft Orbit and Attitude Systems—Mission Geometry; Orbit and Constellation Design and Management*, Space Technology Library, Microcosm, Inc., El Segundo, CA, and Kluwer Academic, Dordrecht, The Netherlands, 2001, Chap. 10.

⁹London, H. S., "Second Approximation to the Solution of the Rendezvous Equations," *AIAA Journal*, Vol. 1, No. 7, 1973, 1963, pp. 1691–1693.

¹⁰Der, G. J., and Danchick, R., "An Analytical Approach to Optimal Rendezvous Using the Der–Danchick Equations," AAS/AIAA Astrodynamics Specialist Conference, Paper 97-647, Aug. 1997.

¹¹Sparrow, G. W., and Price, D. B., "Derivation of Approximate Equations for Solving the Planar Rendezvous Problem," NASA TN-4670, 1968.

¹²Clarke, S. F., and Sedej, D. T., "Rendezvous/Proximity Operations Workbook," Advanced Training Series, NASA Johnson Space Center Document RNDZ 2102, March 1983.

¹³"Flight Procedures Handbook—Proximity Operations," NASA Johnson Space Center, Document JSC-10566, Nov. 1982.

C. A. Kluever
Associate Editor

Low-Cost Small-Satellite Delivery System

Frederick W. Boltz*

Launch Vehicle Technology, Sunnyvale, California 94087

Introduction

DESIGN studies are being funded for a low-cost, small-satellite launcher with the capability of delivering a 110-lb payload to low Earth orbit.¹ Contracts have been awarded to three teams of companies (airframers, engine makers, and rocket builders) participating in the Responsive Access Small Cargo Affordable Launch (RASCAL) project. The concept being pursued is development of a new airbreathing carrier aircraft with a "souped up" turbojet engine (as a reusable first stage) to boost an expendable two-stage rocket to an altitude of about 90,000 ft and a speed of about Mach 4. Then, after coasting to about 130,000 ft, separation of the rocket from the boost vehicle would occur, with the rocket continuing its ascent to orbit and the boost vehicle descending into the lower atmosphere for recovery and reuse. An important factor in any air-launch concept is providing independence from use of a dedicated launch facility with a significant saving in ground support costs. Along with enabling rapid delivery of military satellites to orbit, the goal of the RASCAL project is to have launch on short notice (within 24 h) and at a cost of no more than \$22,000 per pound of payload. It is anticipated that the gross takeoff weight of the boost vehicle would be about 22,000 lb, including 6000 lb for the expendable rocket.

At the present time the Pegasus XL is the only space launch vehicle in the entire U.S. inventory² that is air launched. It is a stretched version of the earlier Pegasus vehicle, which was also air launched but had less performance. The Pegasus XL is a three-stage, solid-propellant rocket with a delta wing attached to the first

Received 5 March 2002; revision received 4 June 2002; accepted for publication 21 June 2002. Copyright © 2002 by Frederick W. Boltz. Published by the American Institute of Aeronautics and Astronautics, Inc., with permission. Copies of this paper may be made for personal or internal use, on condition that the copier pay the \$10.00 per-copy fee to the Copyright Clearance Center, Inc., 222 Rosewood Drive, Danvers, MA 01923; include the code 0022-4650/02 \$10.00 in correspondence with the CCC.

*Aerospace Engineer; currently Senior Consultant, Knowledge Systems Design, Inc., Newport Beach, CA 92663. Senior Member AIAA.